Proceedings of the 9th International Conference on Aluminium Alloys (2004)
Edited by J.F. Nie, A.J. Morton and B.C. Muddle

Simulation of Fatigue Behaviour in Fusion Welded 2024-T351

F. Lefebvre[1], G. Serrano[2], S. Ganguly[3], I. Sinclair[1]

[1]Materials Group, School of Engineering Sciences, University of Southampton, Southampton, UK
[2]Cranfield University, Cranfield, UK
[3]Department of Materials Engineering, The Open University, Milton Keynes, UK

Keywords: short crack, modelling, fatigue, welding

Abstract

A model has been developed to predict short crack fatigue life in the fusion zone of Metal Inert Gas (MIG) welded 2024-T351, based on the observed propensity for complex, multiple cracking processes in this region. To initiate cracks, a Monte-Carlo method has been used, based on the probability of initiation at interdendritic defects derived from the experimental observations. Short crack propagation simulation has been achieved via a microstructurally sensitive approach using continuous dislocation distribution methods. Different geometrical conditions to define crack shielding or crack coalescence have also been identified, along with a first order estimate of crack closure effects and associated influences of residual stress on crack growth. In the regime of specific interest here (crack growth to 1mm total length), good correlation is shown between measured and predicted fatigue performance.

1. Introduction

Recent developments within the commercial aircraft industry are have been focused on both manufacturing cost and weight savings, with significant attention being focused on advanced joining techniques for high strength aluminium alloys [1]. However, few studies of short crack fatigue behaviour have been carried out on such welded materials. The aim of the present study has been to develop appropriate micromechanical understanding and engineering modelling approaches to predict short crack growth life in a welded structure, particularly in terms of crack growth to a 1mm defect size.

2. Material and Experimental Techniques

Butt welded samples were studied in commercial 13mm gauge plane of the standard airframe aluminium alloy, 2024-T351 (solutionised, stretched and naturally aged). The material was welded parallel to the L-direction (i.e. rolling direction) using the Metal Inert Gas welding technique. Samples were welded horizontally in two passes, with basic process details as presented in Table 1.

Table 1: Weld process parameters [2]

Method	Filler wire	Current	Voltage	Welding speed
MIG	2319	268 A	24.3 V	450 mm/min

Short crack fatigue testing was carried out on an Instron 8501 servo-hydraulic machine. Tests were performed parallel to the weld line using three point bend coupons: samples were approximately 100mm long (i.e. parallel to the weld), and 90mm wide (perpendicular to the weld), see Figure 1. Given the fusion zone width of ~12mm, the central test gauge of the weld (i.e. directly over the central roller) may be seen to be approximately 3 times this distance from the cut edges of the sample. Top and bottom surfaces of the samples were skimmed by ~2.5mm from the parent plate surfaces. Loading was applied to the surface of the second weld pass. Constant amplitude sinusoidal cycling was used at a frequency of 15Hz and an R-ratio of 0.1. The top surface (the surface to be fatigue loaded) of all specimens was polished to a 0.02µm finish (using OPS[†], alumina suspension). Crack growth behaviour up to 1mm was monitored by taking acetate replicas of the specimen surfaces at frequent intervals at the maximum applied stress level and then considered by backtracking through the replica record. The analysis of Scott and Thorpe [3] was used to calculate nominal stress intensities levels assuming a semi-circular crack profile.

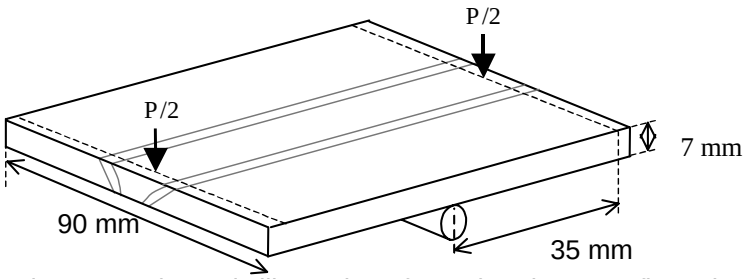

Figure 1: Schematic illustration of 3-pt. bend test configuration

3. Experimental Results

Overall fatigue performance of the MIG welds is illustrated in Figure 2 in terms of stress amplitude-life curves (S-N curves), along with results for the parent plate tested with the same surface preparation and load geometry. It may be seen that the weld results fall below those of the present parent plate tests (by a factor of ~4 in fatigue life). It may be noted that relative performance of the welds falls off significantly at lower stress levels, with the weld results showing a distinctive linear (in logarithmic scale) performance curve.

Crack initiation and early growth were dominated by the fusion zone. It was found that two kinds of weld defect were predominantly present: elongated interdendritic defects of the order of 10 to 50µm, and gas bubbles of the order of hundred's of micrometers. The more acicular but smaller interdendritic pores were measured to be statistically most damaging in terms of crack initiation [2], see Figure 3. The limited incidence of crack initiation from the larger bubble defects may be seen qualitatively from Figure 3(b) in particular. EBSD observations have been carried out to assess the general microstructure and to investigate if crack initiating pores may exhibit a damaging co-location effect with grain boundaries, although no evidence of such additional microstructural contributions to crack initiation was found. Multiple crack initiations were clearly observed in the fusion zone (Figure 3(b)) leading to frequent crack-crack interactions, particularly crack coalescence and stress shielding [2].

[†] Trade names of Struers LTD

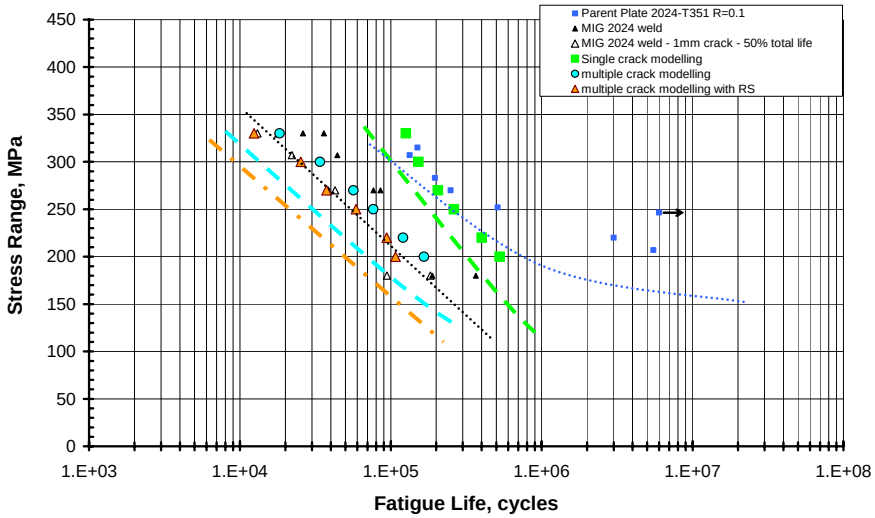

Figure 2: Fatigue life data for the MIG weld and the parent plate 2024. Prediction are also shown of fusion zone fatigue life based on single crack modelling and multiple crack modelling of the fusion zone with or without residual stress (RS) influence.

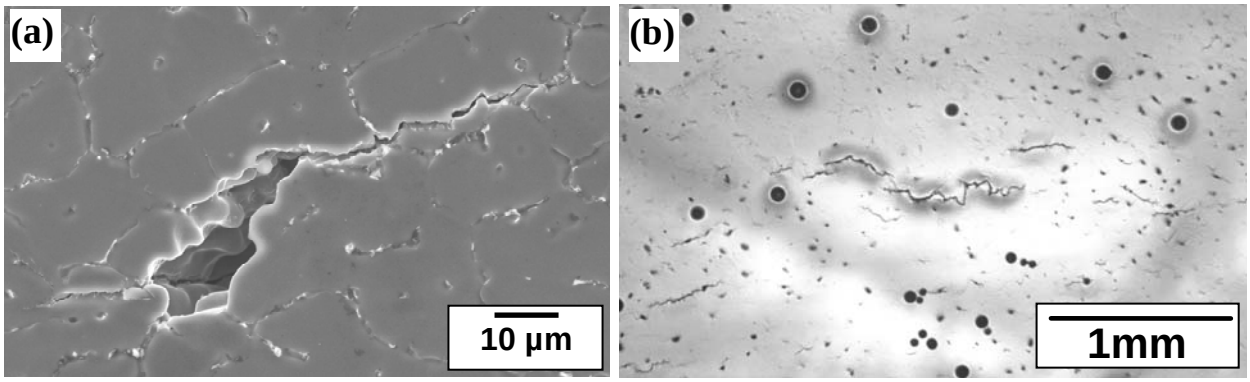

Figure 3: Crack initiation observed in the MIG fusion zone: (a) SEM micrograph of interdendritic pore and associated cracks, (b) optical macrograph of multiple crack initiation at $N/N_f=0.3$, and $\Delta\sigma = 270MPa$.

4. Modelling Approach

A model has been developed to predict the fatigue life of the MIG fusion zone materials based on statistical measurement of pore initiation probability. Modelled pore distributions were identified directly from microstructural imaging. Pores were approximated as ellipses of different aspect ratios, angles to the load axis and sizes (major and minor axes). Ellipse extremities are identified as key crack initiation sites. To initiate cracks, a Monte-Carlo method has been used based on the probability of initiation from each individual pore as a function of its size and shape, as derived from the experimental observations. Cracks are considered to initiate at the start of the fatigue simulations (in the first cycle), as seen experimentally. Initiated cracks are allowed to grow by a defined number of cycles according to a short crack growth model (see below) as a function of their current stress intensity level. Surface crack stress intensity factor levels were calculated using the Scott and Thorpe relationships [3] and initial pore shape effects are ignored.

In terms of growth modelling, propagation behaviour was based on a microstructure sensitive approach using continuous dislocation distribution methods, as reported by Edwards and Zhang [4]. Zhang & Edwards consider that, based on experimental evidence, short crack growth rates are directly related to active plastic zone size. They note that the relatively large plastic deformation zone associated with small fatigue cracks may explain

their fast growth rates compared to long cracks. As such the intrinsic decelerations and accelerations of small cracks are considered in terms of the effect of grain boundaries on plastic deformation ahead the crack tip. In the present crack growth simulation, the main principles are as follows:

(i) When the plastic zone ahead of a crack tip is not blocked by the forthcoming grain boundary, the plastic zone size is calculated via the method developed by Bilby, Cottrell and Swinden [5] for continuous distribution of infinitesimal dislocations with a uniform applied stress. The plastic zone may be calculated from the condition of vanishing dislocation density at the extremity of the zone [6].
(ii) If the plastic deformation is blocked, and if the stress at the dislocation source in the next grain is not superior to a critical stress (stress to overcome the grain boundary), the plastic zone size is assumed to be the distance between the crack tip and the next grain boundary.
(iii) Once the grain boundary is overcome, the plastic zone in the next grain is calculated according again to the dislocation distribution method.

It is then assumed that growth rates are related to the plastic zone size ahead of the crack tip via an exponential equation of a Paris Law form. In terms of experimental crack growth data used to define the material constants, it is clearly ideal to have growth data for MIG fusion zone material in a residual stress-free condition, and a number of individual cracks that can be monitored without crack-crack interactions. In terms of the latter condition, it may be noted that the MIG fusion zone material is problematic due to its high intrinsic susceptibility to multiple crack initiation (high defect density). As such short crack fatigue data from small ‘sub-sized’ fusion zone samples (3x1.5mm in cross section) from a low defect Variable Polarity Plasma Arc weld have been used [3]. Given the small size of these samples and the fact that only a few cracks form in each test, is assumed the growth rate data are reasonably representative of residual stress free, individual crack growth processes. This data was therefore been used as the best available approximation to intrinsic short crack growth behaviour in the MIG fusion zone, bearing in mind: (a) the same filler wire was used (2319), (b) a similar equiaxed grain structure was present in each, (c) similar hardness levels and DSC traces were obtained [3].

Crack-crack interactions are considered, with different conditions to define the incidence of crack shielding or crack coalescence. Finite element analysis, analytical modelling, and experimental observations of fatigue behaviour in multiple crack fields has been published previously [7-9], highlighting the roles of plastic zone size, crack positioning, and crack driving forces in crack-crack interactions [7-9]. The crack-crack interaction conditions considered in the present modelling are presented schematically in Figure 4. As suggested by Hünecke and Schöne [10], it is assumed that stress shielding leads to simple crack tip arrest: when a crack is arrested, it does not have the possibility to grow further again. Shielding interactions are treated as a severe “brick-wall” effect: a notional “shielding area” associated with a crack is considered as a circle of diameter equal to the crack length. The red circles in Figure 4 illustrate different shielding areas. For a given crack, if the shielding area intercepts one or both crack tips of another crack, then the corresponding tips are considered to be shielded from any further growth. In terms of coalescence, a “coalescence area” is defined as a circle of radius equal to the nominal plastic zone size, based on the Irwin approximation for plane stress conditions [11]. In Figure 4, the green circles at the crack tips represent different coalescence areas. For a given crack, if the coalescence area intercepts a coalescence area of another crack, the cracks are considered to spontaneously coalesce (i.e. zero cycles to cross the separation distance

associated with the plastic zone dimensions). A new crack is then considered with a length given by the distance between the two remaining tips.

Crack growth and crack-crack interaction simulation are repeated until one of the cracks (or coalesced group of cracks) achieves a pre-determined length of 1 mm corresponding to a notional short crack regime limit. In the actual MIG weld tests, the time to form 1mm cracks (or 1mm coalesced groups of cracks) was seen to correspond to approximately 50% of total fatigue life. Figure 5 presents an example of a simulated area (1.2mmx1.4mm) with associated crack initiation and growth for a stress level of 270 MPa after 79000 cycles. Crack interactions may be seen: i.e. crack shielding and crack coalescence. Different simulated areas were considered to achieve a statistically representative sample of defect population, with an area of ~ 7 x 1.5mm (representing approximately half a fusion zone width) being found to represent a consistent microstructural sample size for the present modelling purposes.

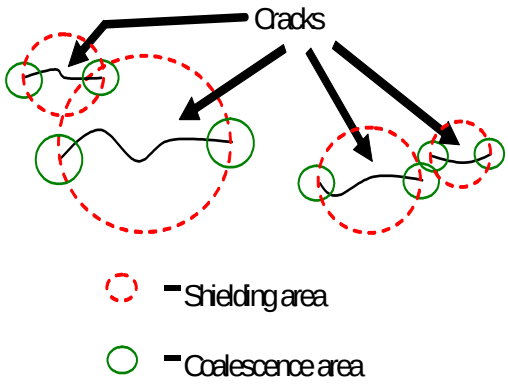

Figure 4: Schematic illustration of crack.

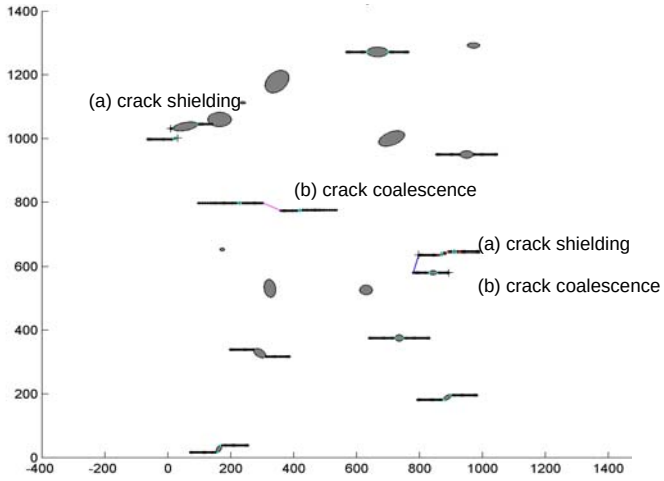

Figure 5: Pore distribution with the associated crack initiation and growth for a stress level of 270MPa after 79000 cycles. Crack interaction may be seen at: (a) crack shielding and (b) crack coalescence.

As with all welding processes, significant residual stress levels are generated in the present weld samples. Residual stresses measurements have been carried out on machined and electro-polished fatigue specimen surfaces (to remove potential artefacts of mechanical preparation). Measurements have been carried out using a “Bruker” laboratory X-ray machine, with a (331) reflecting plane, and confirmed against synchrotron diffraction measurements carried out at the ESRF. Specimens were examined before loading, and after a single load cycle (to a stress level of 270MPa) to assess relaxation effects associated with any initial deformation. Peak stress longitudinal levels of 50MPa were identified within the fusion zones of the present fatigue samples (i.e. after cutting and skimming from the original welded state).

In first approximation, the influence of residual stress on fatigue has been expressed in terms of crack closure effects on propagation, with elastic superposition arguments being used to express residual stresses as an effective increase of R-ratio. In the first instance, baseline crack closure conditions have been estimated from the sub-sized coupon tests by noting that closure levels must tend to zero for cracks of decreasing length, and that at the point on a conventional da/dN plot where short and long crack data merge, closure conditions in the short cracks must approach those of the long. Linear interpolation is then used to span these two conditions.

5. Discussion and Conclusion

Figure 2 presents predictions of fatigue life for three versions of the current model for a final total crack length of 1mm, based on: (i) a notional single crack growing from a pre-defined defect of 20µm length, i.e. characteristic of the typical crack initiating particle size in parent plate, (ii) a simulated weld area with multiple cracking but no residual stress influence, and (iii) a simulated weld area with multiple cracking, with residual stress influence. It may be seen that both versions of the model representing the weld microstructure provide a reasonable approximation of the weld behaviour (i.e. measured fatigue life to 1mm crack length). Model results incorporating residual stresses are in fact seen to fall very close to the experimental data: - given the approximations of the model such close numeric accuracy should be seen as slightly fortuitous. It may however be concluded that the present integration of crack initiation, propagation and interaction effects, do provide a good approximation of weld behaviour, with residual stresses appearing to have a relatively minor influence on fatigue life, consistent with the present consideration of short crack behaviour where closure effects are expected to be limited (cf. long cracks).

Acknowledgements

The authors wish to thank Airbus UK for materials supply and financial support, and the EPSRC for financial support.

References

[1] Woodward, N.J., I.M. Richardson, and A. Thomas, Variable polarity plasma arc welding of 6.35 mm aluminium alloys: parameter development and preliminary analysis. Science and Technology of Welding and Joining, 2000. 5(1): p. 21-25.

[2] Lefebvre, F., Micromechanical assessment of fatigue in airframe fusion welds (PhD thesis), in School of Engineering Sciences, Material Research Group. 2003, University of Southampton: Southampton.

[3] Scott, P.M. and T.W. Thorpe, A critical review of crack tip stress intensity factors for semi-elliptic cracks. Fatigue of Engineering Materials and Structures, 1981. 4(4): p. 291-309.

[4] Edwards, L. and Y.H. Zhang, Investigation of Small Fatigue Cracks .2. A Plasticity Based Model of Small Fatigue-Crack Growth. Acta Metallurgica Et Materialia, 1994. 42(4): p. 1423-1431.

[5] Bilby, B.A., A.H. Cottrell, and K.H. Swinden, The spread of plastic yield from a notch. Proc. Roy. Soc. Lond., 1963. 272A: p. 304-314.

[6] Navarro, A. and E.R. de los Rios, Short and long fatigue crack-growth - a unified model. Philosophical magazine A - Physics of condensed matter structure defects and mechanical properties, 1988. 57: p. 15-36.

[7] Joyce, M.R., Fatigue of aluminium linings in plain automative bearings (PhD Thesis), in School of engineering sciences, Materials Research Group. 2000, University of Southampton: Southampton. p. 243.

[8] Chen, E.Y., L. Lawson, and M. Meshii, The effect of fatigue microcracks on rapid catastrophic failure in Al-SiC composites. Materials Science and Engineering A, 1995. 200: p. 196-206.

[9] Hünecke, J., et al. Observation and simulation of short crack behaviour in a low Carbon Stell under constant amplitude loading. in Conference Materials week. 2001. Munich.

[10] Hünecke, J. and D. Schöne. Life prediction by observation and Simulation of short crack behaviour in a low carbon steel. in Symposium of fatigue testing and analysis under variable amplitude loading. 2002. Tour (France): ASTM.

[11] Hünecke, J. and D. Schöne. Simulation of the short crack behaviour of the low carbon steel SAE1017 under fatigue loading. in Conference Materials week. 2002. Munich.